# DNS OF TURBULENT PIPE FLOW IN A TRANSVERSE MAGNETIC FIELD

**Shin-ichi Satake**
Dept. of Mech. Intellectual Sys. En., Toyama University
3190 Gofuku , Toyama city, Toyama, 930-8555, JAPA N
ssatakel@eng.toyama-u.ac.jp

**Tomoaki Kunugi**
Dept of Nuclear Eng., Kyoto University
Yoshida, Sakyo, Kyoto, 606-8501, JAPAN
kunugi@nucleng.kyoto-u.ac.jp

**Sergey Smolentsev**
UCLA, Department of Mechanical and Aerospace Engineering
Los Angeles CA 90095-1597
sergey@fusion.ucla.edu

## ABSTRACT

A direct numerical simulation (DNS) of turbulent pipe flow with a constant transverse magnetic field has been carried out to grasp and understand the effects of electromagnetic suppression of turbulence caused by a constant transverse magnetic field. In this study, the Reynolds number based on a bulk velocity and a pipe diameter was set to be constant; $Re_b$ = 5300. The magnetic field at $Ha$ = 5, 10, 20, taken from the electrical potential equation was applied to a constant transverse magnetic field. In the flow field, the Lorenz forces act on radial and circumferential components of momentum equation with cylindrical coordinate. The number of computational grids used in this study was 256 x 128 x 128 in the $z$-, $r$- and $\phi$-directions, respectively. The turbulent quantities such as the mean flow, turbulent stresses and the turbulent statistics were obtained via present DNS. The mean velocity and turbulent intensities distributed circumferentially and is damped quickly near the top of the pipe ($\phi$ = 0). The reason of this behavior can be considered that the Hartman layer drastically changes to the circumferential direction.

## INTRODUCTION

There is considerable renewed interest in the area of Magneto hydrodynamics (MHD), in the area of MHD turbulent control and also in conceptual designs of proposed blankets of fusion reactors. The flow fields such as the areas are turbulent shear flow in a transverse magnetic field. In a pipe flow with a transverse magnetic field, the velocity profile exhibited the Hartmann flattening at the top of the pipe ($\phi$ = 0 ) and also showed that the profiles become more rounded in the near wall region at $\phi$ = $\pi$ /2. A relative decrease in the turbulent kinetic energy subjected to the Hartmann layer flattening at $\phi$ = 0 is observed. These phenomena become more remarkable with increase of Hartmann number.

An extensive experimental work was done by Gardner and Lykoudis (1971) for the turbulent pipe flow in a transverse magnetic field. Distribution of mean velocity and fluctuation were measured in the pipe flow with various strength of magnetic field.

A direct numerical simulation (DNS) of turbulent pipe flow with axial and azimuthal magnetic fields and was performed by Olrandi (1996). He studied that the effect of the orientation of magnetic filed and found in both cases the drag reduction is achieved.

In this paper, the DNS is performed for the turbulent pipe flow with a transverse magnetic field. The turbulent statistics for the friction coefficients are predicted and compared with theoretical correlation (Sherclif, 1956). Furthermore, also presented are predictions for the mean velocity and fluctuation, which is obtained for each degree in the azimuthal direction.

## NUMERICAL PROCEDURE

The DNS code with cylindrical coordinates can numerically solve the continuity and momentum equations using the radial momentum flux formulation. A second-order finite volume discretization scheme is applied to the spatial derivatives on a staggered mesh system in order to avoid a singularity at the center axis of the pipe center. The incompressible Navier-Stokes and continuity equations described in cylindrical coordinate are integrated in time by using the fractional-step method. The second-order Crank-Nicholson scheme is applied to the radial direction terms treated implicitly and a modified third-order Runge-Kutta scheme is used for other terms explicitly. In our previous study regarding the non-MHD turbulent pipe flow (Satake and Kunugi, 1998), this DNS code has been shown in good agreement

with the existing DNS results. In this study, the magnetic field can be calculated by solving the electrical potential equation instead of the Maxwell equations. The equation is solved using Fourier trans form and tridiagonal matrix technique.

## COMPUTATIONAL CONDITIONS

The computational domain is shown in Figure 1. The computational parameters are given in Table 1. The Reynolds number based on the bulk velocity, viscosity and the pipe diameter ($D$) is assumed to be 5300. Uniform mesh spacing is applied to the circumferential ($\phi$) and the streamwise ($z$) directions. As for the radial direction ($r$), non-uniform mesh spacing specified by a hyperbolic tangent function is employed. The number of grid points is 256 x 128 x 128 in the $z$-, $r$- and $\phi$ -directions, respectively. The periodic boundary conditions are adopted for streamwise and circumferential direction. The all velocity components imposed the non-slip condition at the wall. $\boldsymbol{B}_0$ is the transverse magnetic field. Neumann condition on the electrical potential is adopted at the wall. The computational domain is shown in Figure 1. The Hartmann number ($Ha = \boldsymbol{B}_0 R\,(\sigma/\rho\nu)^{1/2}$) based on $\boldsymbol{B}_0$ the magnetic field, $\nu$ the kinematic viscosity, $\sigma$ the electrical conductivity and the pipe radius $R$ are assumed to be 5, 10, 20.

## RESULTS AND DISCUSSION

Figure 2 shows a comparison of present skin friction with Shercliff's analytical solution. It can be seen that the skin friction at $Ha$ =5, 10 are smaller than Non MHD case. But at $Ha$=20, skin friction is lager than Non MHD case and the curve fit of calculated skin friction closely matches Shercliff's analytical solution for laminar pipe flow. These results showed that the skin friction is slightly smaller than Non MHD case when Hartmann number is low

Mean velocity profiles with MHD at three angles ($\phi$ = 0, $\pi$/4, $\pi$ /2) and without via DNS are shown in Fig. 3. Regarding the results with MHD obtained from the DNS, the Lorentz force near the wall region due to circumferentially magnetic fields increases the velocity at $\phi = \pi$ /2. This indicates that the increase near wall region at $\phi$ = 0 is primary caused by the so-called "Hartman effect". That is, the Hartmann effect flattens the velocity profile and decrease with increasing the angle. At $\phi = \pi$ /2, the profiles become more rounded than the zero-field profile. These effects are due to the fact that accelerations the flow near wall at $\phi$ = 0, but not at $\phi = \pi$ /2. Gardner and Lykoudis (1971) found that the effect is distributed in circumferential direction. Note that the DNS for the ordinary pipe flow without MHD is smaller at the whole region as shown in same figure.

Figure 4 shows the distributions of streamwise velocity fluctuations. It is interesting that the streamwise component near the wall region obtained by the DNS with MHD is most decreasing at $\phi = \pi$ /2, and that at all angles is smaller than the DNS without MHD.

Figure 5 shows the distributions of radial velocity fluctuations. The values decrease at the pipe center. It is natural that the effect of magnetic suppression $\phi$ =0 is especially strong in the radial component.

Figure 6 shows the distributions of azimuthal velocity fluctuations. The distribution at the pipe center shows the similar trend to the radial component. Thus, the turbulence behavior in the DNS with MHD tends to be more isotropic than that without MHD, and the behavior of the radial and circumferential velocity fluctuating components near wall region is more damped with increasing angle, is obtained the peak value at $\phi = \pi$ /2.

Figure 7 (a)(b)(c) show the contour of the low-speed streaky structures. They are normalized by $\nu$ and averaged $u_\tau$. The volume visualized is obtained as from full computational volume. In non MHD case, approximately ten streaks can be counted in the azimuthal direction in Fig. 7(a). If the length is nondimensionalized with friction velocity and the kinematic viscousity, the width of circumference of the wall, is about 1130. Thus the average spacing of the streaks is about 100-150.

However, in low Hartmann number ($Ha$= 10), the location of the skreaky structures observed locally and the number of streaks are less than that without MHD. Almost structures located at $\phi = \pi$ /2, correspond to the rounded profile in the mean velocity profile. The effect of magnetic field on the angle is evident. The suppression in the streamwise velocity fluctuation at $\phi$ =0 shows a similar trend in Fig.4. At $Ha$= 20, the strucutres do not appear and the weakly values ($u^+$<-0.28) remain only at the center of pipe and the near wall region at $\phi = \pi$ /2.

## SUMMARY

The DNS for the turbulent pipe flow with a constant transverse magnetic field was carried out. It is confirmed by the present DNS that the remarkable reduction of the turbulence at $\phi$ = 0 is due to the magnetic field change of circumferentially. The turbulent fluctuation decreased mostly appears at $\phi$ = 0.

The decreasing also observed in the streaky structures from visualization. Some features of electromagnetic suppression by the transverse magnetic field can be predicted via this DNS. More detailed results, turbulent kinetic energy and Reynolds stress budgets for each Hartmann number cases and discussion will be reported in the presentation.

**References**

Gardner, R.A. and Lykoudis, P.S., 1971,"Magneto-fluid-mechanic pipe flow in a transverse magnetic field. Part1. Isothermal flow," J. Fluid Mech. Vol.47, part 4, pp. 737-764.

Orlandi, P., 1996, "Drag reduction in turbulent MHD pipe flows," CTR, Proc of the summer program 1996, pp. 447-456.

Shercliff, J., 1956,"The flow of conducting fluids in circular pipes under transverse magnetic fields," J. Fluid Mech., ol.1, pp. 644-666.

Satake, S. and Kunugi, T., 1998,"Direct numerical simulation of turbulent pipe flow," Bulletin JSME Vol.64, pp. 65-70.

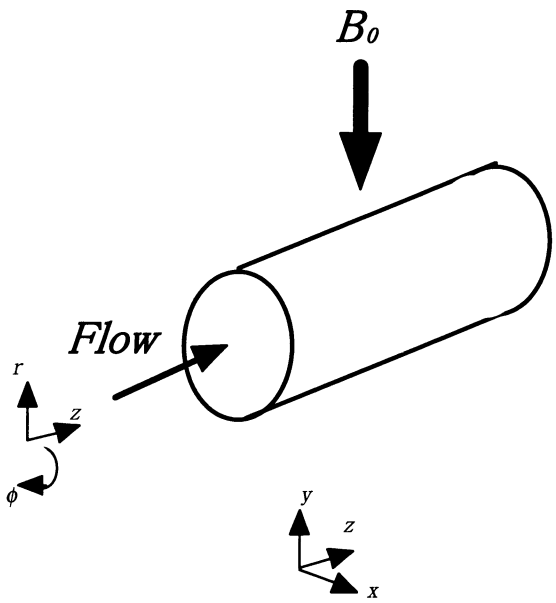


Figure 1 Computational domain

Table 1 Hartmann number and Reynolds number

| $Ha$ | $Re_b$ | $Re_\tau$ |
|---|---|---|
| 0 | 5300 | 180 |
| 5 | 5300 | 176 |
| 10 | 5300 | 160 |
| 20 | 5300 | 192 |

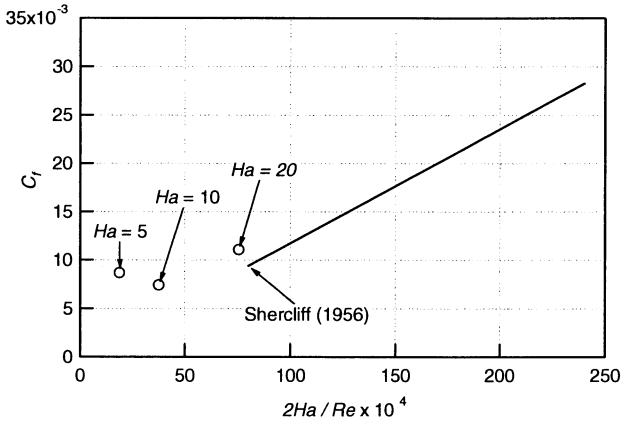


Figure 2 Skin friction coefficients

(a) $\phi = 0$

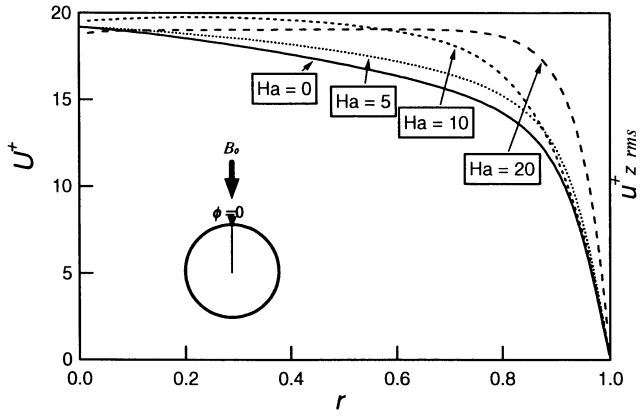


(b) $\phi = \pi/4$

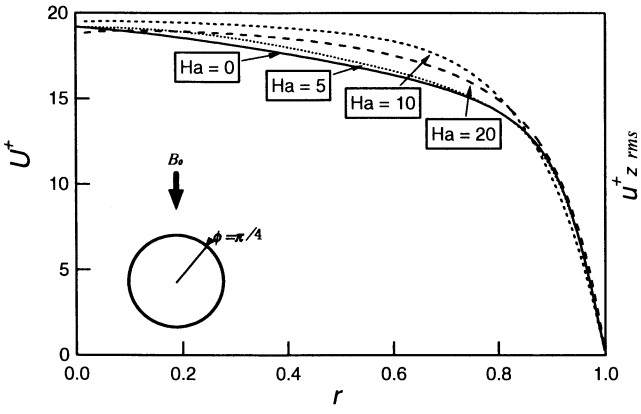


(c) $\phi = \pi/2$

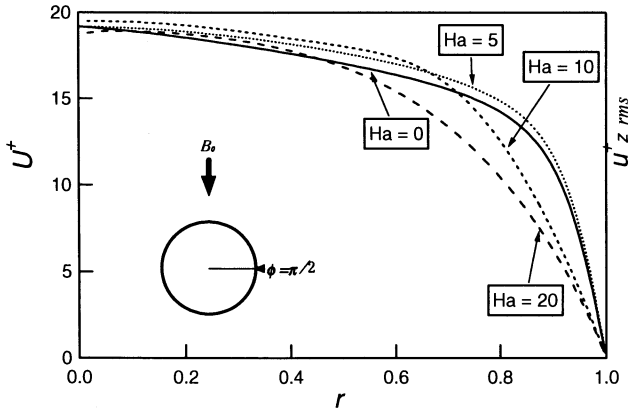


Figure 3 Mean velocity profiles: (a) $\phi = 0$, : (b) $\phi = \pi/4$, : (c) $\phi = \pi/2$.

(a) $\phi = 0$

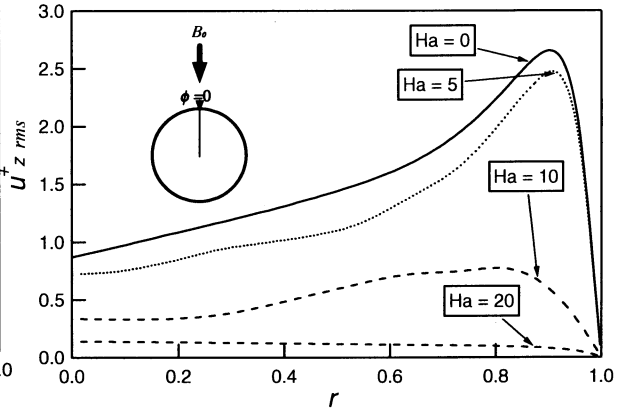


(b) $\phi = \pi/4$

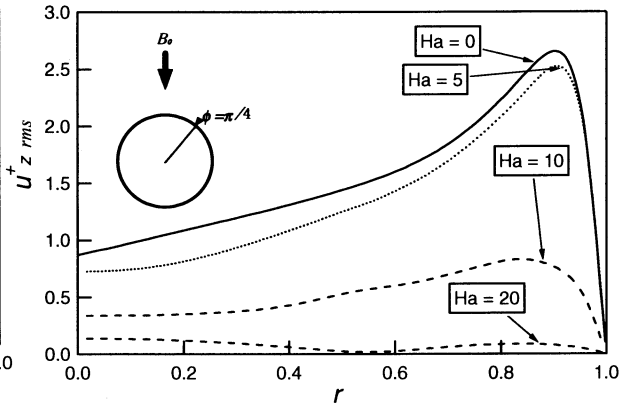


(c) $\phi = \pi/2$

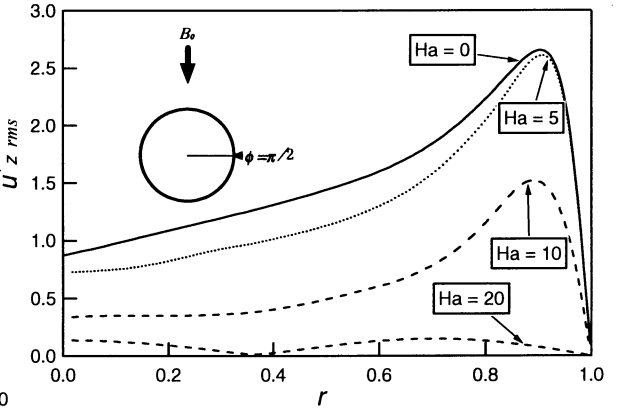


Figure 4 Streamwise velocity fluctuations: (a) $\phi = 0$, : (b) $\phi = \pi/4$, : (c) $\phi = \pi/2$.

(a) $\phi = 0$

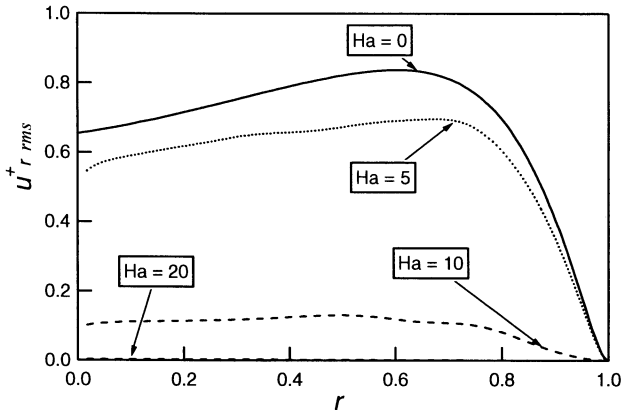


(b) $\phi = \pi/4$

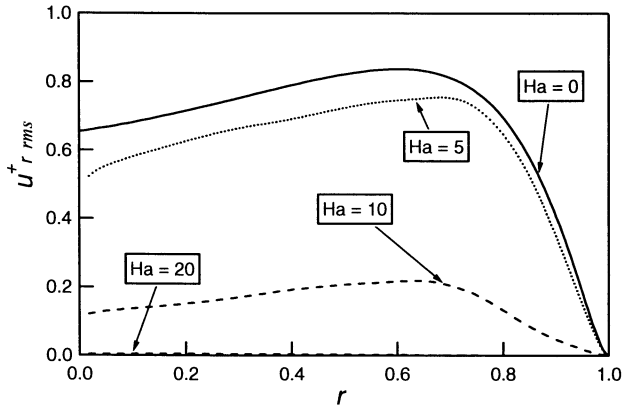


(c) $\phi = \pi/2$

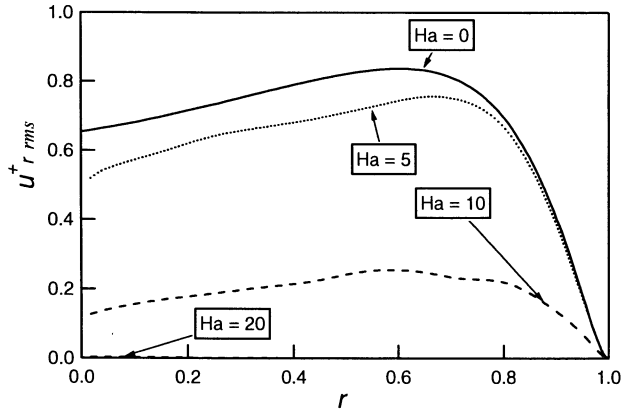


Figure 5 Radial velocity fluctuations: (a) $\phi = 0$, : (b) $\phi = \pi/4$, : (c) $\phi = \pi/2$.

(a) $\phi = 0$

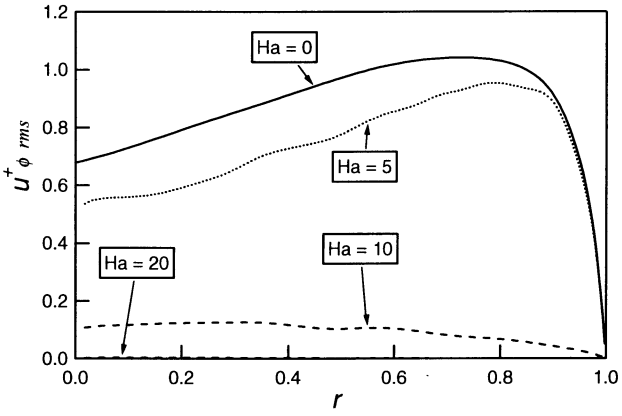


(b) $\phi = \pi/4$

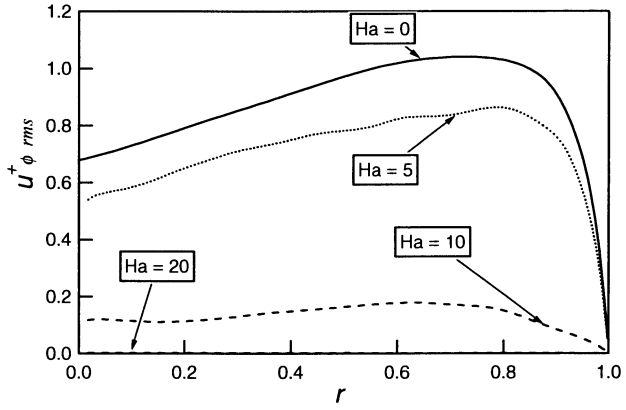


(c) $\phi = \pi/2$

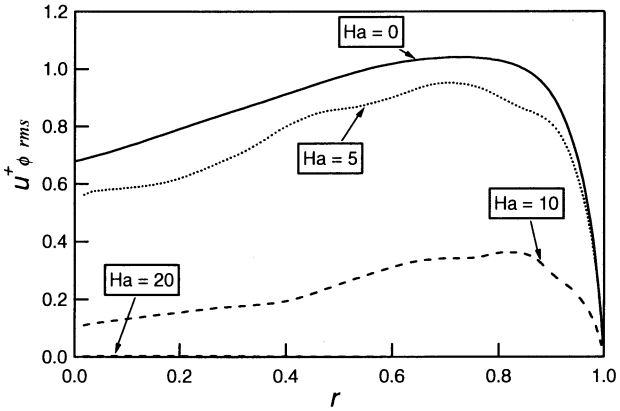


Figure 6 azimuthal velocity fluctuations: (a) $\phi = 0$, : (b) $\phi = \pi/4$, : (c) $\phi = \pi/2$.

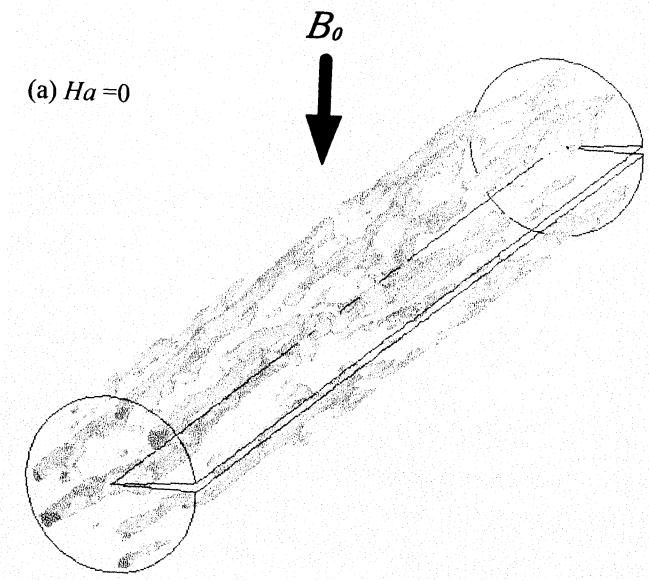


(a) $Ha$ =0

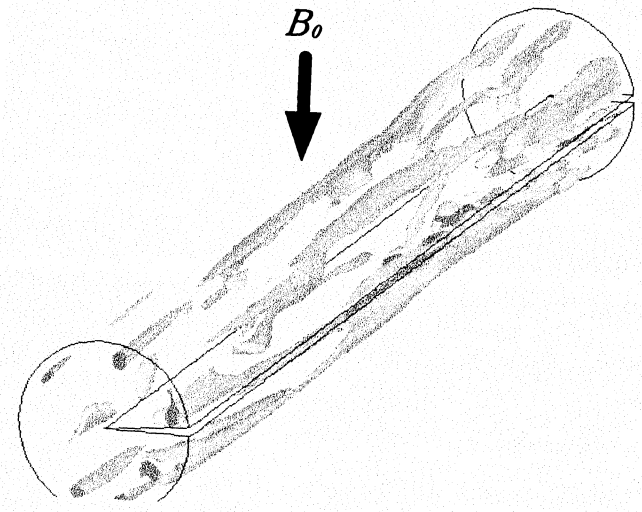


(b) $Ha$ =10

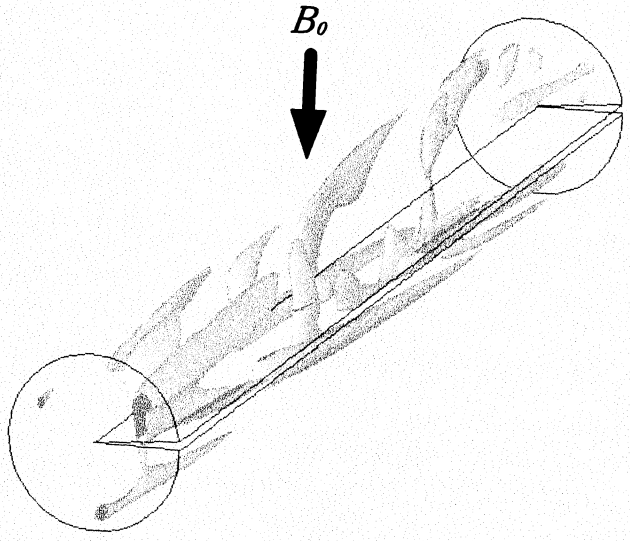


(c) $Ha$ =20

Figure 7 3-D contour surface low-speed streak; (a) Non-MHD, Grey: Low-speed streak ($u^+$<-3); (b) $Ha$=10, Grey: Low-speed streak ($u^+$<-1.5); (c) $Ha$=20, Grey: Low-speed streak ($u^+$<-0.28)